Electronic Supplementary Material (ESI) for Chemical Communications.

Electronic Supplementary Information (ESI)

Efficient and Selective Carbon-Carbon Coupling on Coke-Resistant PdAu Single-Atom Alloys

Romain Réocreux,‡[a] Matthew Uhlman,‡[b] Theodore Thuening,[b] Paul Kress,[b] Ryan Hannagan,[b] Michail Stamatakis[a] and Charles Sykes[b]

[a] Thomas Young Centre and Department of Chemical Engineering, University College London, Roberts Building, Torrington Place, London WC1E 7JE, United Kingdom.

[b] Department of Chemistry, Tufts University, Medford, Massachusetts 02155, United States.

‡These authors equally contributed to the work

Methods

Temperature Programmed Desorption (TPD)

All experiments were performed in two ultrahigh vacuum (UHV) chambers with a base pressure of < 1×10^{-10} mbar. Two Au(111) single crystals (Princeton Scientific) were cleaned using Ar^+ sputtering cycles (1.5 keV, 10 µA) followed by annealing to 725 K. Stepped Au(111) was prepared the same way, but without the annealing step. Pd was deposited via physical vapor deposition with the crystal held at 380 K using a flux-monitored Omicron Nanotechnology Focus EFM 3 electron beam evaporator. Liquid MeI (Sigma Aldrich, 99.5%) and deuterated MeI (Sigma Aldrich, 99.5%) were purified through freeze-pump-thaw cycles, and monitored for purity via mass spectrometry. The compounds were dosed into the chamber through a high-precision leak valve (Duniway) onto the crystal. TPD experiments were then performed in the UHV chamber equipped with a Hiden quadrupole mass spectrometer with a heating rate of 1 K s^{-1}. Coverages of Pd were calibrated by CO (Airgas, 99.99%) adsorption, as previously reported.[1] STM studies were performed using a low-temperature scanning tunneling microscope (Omicron Nanotechnology) at 5 K with a base pressure < 1×10^{-11} mbar.

Computational Details

All molecular calculations were performed using the periodic DFT approach as implemented in the Vienna *Ab Initio* Simulation Package (VASP) version 5.4.1.[2–4] We used the optB86b-vdW[5–7] to describe the electronic exchange and correlation potentials. The core electrons were treated with the Projected Augmented Wave[8] approach and the valence electronic density was expanded on a plane wave basis set truncated at an energy cut-off of 400 eV. The electronic density was optimized solving the Kohn-Sham equations iteratively until the associated energy reached a tolerance of 10^{-6} eV. The relaxation of the positions of atoms was considered converged for forces less than 10^{-2} eV $Å^{-1}$.

Pristine (111) surfaces were modeled using a 4 layer $p(4\times4)$ slab for Au(111). Only the top two layers were relaxed, keeping the atoms of the bottom two layers fixed at their bulk position (lattice constant of 4.127 Å). To model the highly diluted Pd-doped surface, we substituted one surface Au atom by Pd in the unit cell. The sampling of the Brillouin-zone was performed over a Monkhorst-Pack 7×7×1 k-point mesh.[9]

Since the experimental system exhibits the herringbone reconstruction, the (111) model surface just discussed might not be the most appropriate representation of the real system. To therefore assess the potential limitations of the (111) pristine surface model, 4 layer $p(3\times1)$ Au(211) surfaces were also considered. PdAu(211) models were built from the Au(211) surface, substituting one surface Au with Pd at the step-edge. The sampling of the Brillouin-zone was then performed over a Monkhorst-Pack 11×9×1 k-point mesh.[9]

All intermediates were optimized using the Conjugate Gradient algorithm. Transition states were first approximated using the Climbing-Image Nudged Elastic Band (CI-NEB)[10,11] method and further refined using Quasi-Newton or Dimer methods.[12–14] For each structure, we performed a vibrational analysis (freezing the coordinates of the metal atoms at their optimized position). For transition states, in particular, we verified that they all are first order saddle points in the potential energy surface.

The partition functions (used to evaluate the thermodynamic and rate constants) were estimated within the Harmonic Oscillator approximation. The rotational modes of gas phase molecules were accounted for within the Rigid Rotor approximation. Finally, the temperature dependent rate constants were determined by Transition State Theory (TST) and used as input to the TPD simulations.

The kinetic simulations were performed with the on-lattice kMC code *Zacros* 2.0.[15,16] The Au(111) lattice consists of 15300 sites (5100 top sites and 10200 three-fold sites). When considering PdAu(111) SAA, 153 top sites (to match the experimental 3% surface loading in Pd) have been randomly selected and substituted by Pd top sites (also changing the nature of the 6 neighbouring three-fold sites from Au three-fold sites to mixed PdAu three-fold sites). KMC simulations for PdAu(211) SAA are performed on the same lattice as PdAu(111) changing the DFT activation parameters at the Pd site to the DFT values computed on the (211) slab. The configurations were initiated using a random seeding of methyls on the Pd sites first, and then on the Au sites. Diffusion processes were rescaled for computational efficiency in such a way the event frequency per site thereof is a least 100 times larger than the coupling reaction; for all other events, the original rate constants (as computed from TST) were used. Each curve in Figure 3b corresponds to the average of 8 different simulations with the same initial condition but a different (chosen randomly) integer seed for the random number generator of *Zacros*.

Density Function Theory – Supplementary data

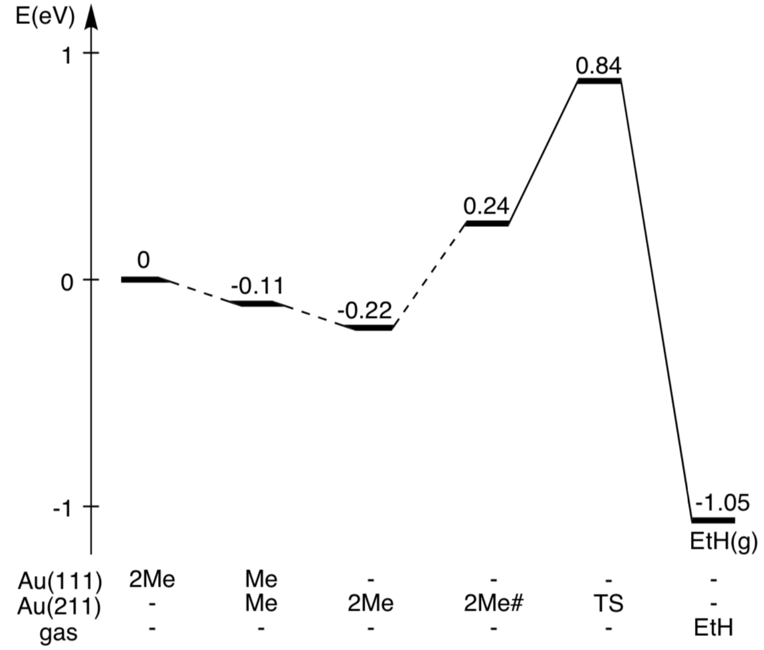

Figure S1. Potential Energy surface of 2 methyls diffusing from Au(111) to Au(211) where they couple to EtH. “2Me#” denotes two methyls that are adsorbed on the same Au atom at the step edge. Dashed lines correspond to diffusion steps for which no transition states were investigated.

Table S1. Structures of various transition states on PdAu and Au surfaces with the associated activation energies in eV

	Bond formation/cleavage	Au	PdAu
(111) surface	C-I anti	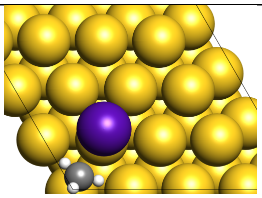 0.99	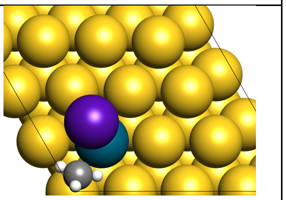 1.01
	C-I syn	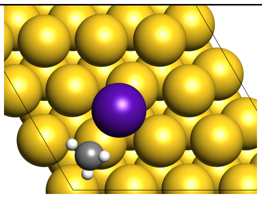 1.24	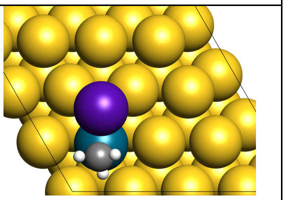 0.97
	C-H	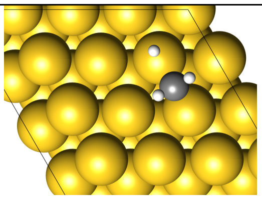 1.79	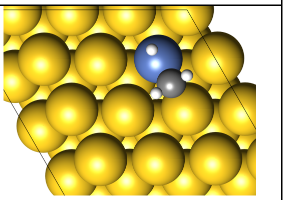 1.27
	C-C	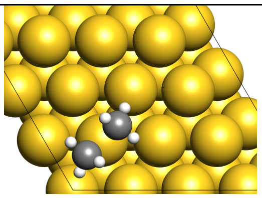 1.51	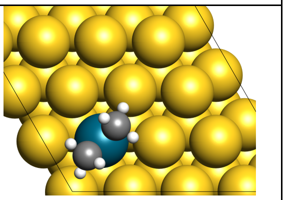 1.12
(211) surface	C-I anti	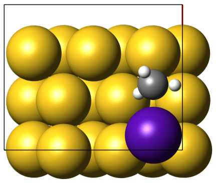 0.35	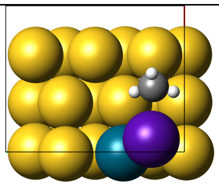 0.44
	C-I syn	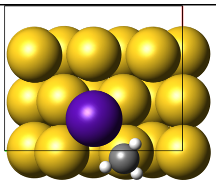 0.94	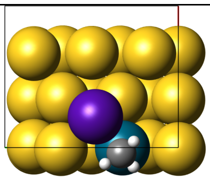 0.67
	C-H	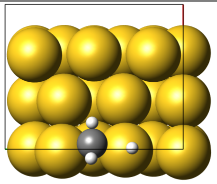 1.36	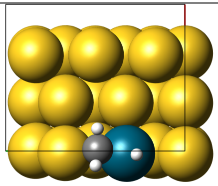 0.94
	C-C	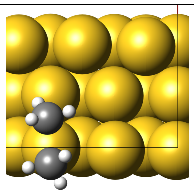 0.97	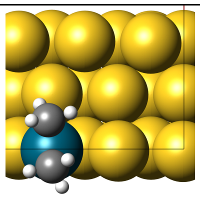 0.45

References

(1) Lucci, F. R.; Darby, M. T.; Mattera, M. F. G.; Ivimey, C. J.; Therrien, A. J.; Michaelides, A.; Stamatakis, M.; Sykes, E. C. H. Controlling Hydrogen Activation, Spillover, and Desorption with Pd–Au Single-Atom Alloys. *J. Phys. Chem. Lett.* **2016**, *7* (3), 480–485. https://doi.org/10.1021/acs.jpclett.5b02400.

(2) Kresse, G.; Hafner, J. Ab Initio Molecular Dynamics for Liquid Metals. *Phys. Rev. B* **1993**, *47*, 558–561. https://doi.org/10.1103/PhysRevB.47.558.

(3) Kresse, G.; Furthmüller, J. Efficient Iterative Schemes for Ab Initio Total-Energy Calculations Using a Plane-Wave Basis Set. *Phys. Rev. B* **1996**, *54*, 11169–11186. https://doi.org/10.1103/PhysRevB.54.11169.

(4) Kresse, G.; Furthmüller, J. Efficiency of Ab-Initio Total Energy Calculations for Metals and Semiconductors Using a Plane-Wave Basis Set. *Comput. Mater. Sci.* **1996**, *6*, 15–50. https://doi.org/10.1016/0927-0256(96)00008-0.

(5) Dion, M.; Rydberg, H.; Schröder, E.; Langreth, D. C.; Lundqvist, B. I. Van Der Waals Density Functional for General Geometries. *Phys. Rev. Lett.* **2004**, *92*, 246401. https://doi.org/10.1103/PhysRevLett.92.246401.

(6) Klimeš, J.; Michaelides, A. Perspective: Advances and Challenges in Treating van Der Waals Dispersion Forces in Density Functional Theory. *J. Chem. Phys.* **2012**, *137*, 120901–120913. https://doi.org/10.1063/1.4754130.

(7) Klimeš, J.; Bowler, D. R.; Michaelides, A. Van Der Waals Density Functionals Applied to Solids. *Phys. Rev. B - Condens. Matter Mater. Phys.* **2011**, *83* (19), 1–13. https://doi.org/10.1103/PhysRevB.83.195131.

(8) Kresse, G.; Joubert, D. From Ultrasoft Pseudopotentials to the Projector Augmented-Wave Method. *Phys. Rev. B* **1999**, *59*, 1758–1775. https://doi.org/10.1103/PhysRevB.59.1758.

(9) Monkhorst, H. J.; Pack, J. D. Special Points for Brillouin-Zone Integrations. *Phys. Rev. B* **1976**, *13*, 5188–5192. https://doi.org/10.1103/PhysRevB.13.5188.

(10) Henkelman, G.; Uberuaga, B. P.; Jónsson, H. A Climbing Image Nudged Elastic Band Method for Finding Saddle Points and Minimum Energy Paths. *J. Chem. Phys.* **2000**, *113*, 9901. https://doi.org/10.1063/1.1329672.

(11) Sheppard, D.; Terrell, R.; Henkelman, G. Optimization Methods for Finding Minimum Energy Paths. *J. Chem. Phys.* **2008**, *128*, 134106. https://doi.org/10.1063/1.2841941.

(12) Henkelman, G.; Jónsson, H. A Dimer Method for Finding Saddle Points on High Dimensional Potential Surfaces Using Only First Derivatives. *J. Chem. Phys.* **1999**, *111*, 7010. https://doi.org/10.1063/1.480097.

(13) Heyden, A.; Bell, A. T.; Keil, F. J. Efficient Methods for Finding Transition States in Chemical Reactions: Comparison of Improved Dimer Method and Partitioned Rational Function Optimization Method. *J. Chem. Phys.* **2005**, *123*, 224101. https://doi.org/10.1063/1.2104507.

(14) Kästner, J.; Sherwood, P. Superlinearly Converging Dimer Method for Transition State Search. *J. Chem. Phys.* **2008**, *128*, 014106. https://doi.org/10.1063/1.2815812.

(15) Nielsen, J.; D'Avezac, M.; Hetherington, J.; Stamatakis, M. Parallel Kinetic Monte Carlo Simulation Framework Incorporating Accurate Models of Adsorbate Lateral Interactions. *J. Chem. Phys.* **2013**, *139* (22), 224706. https://doi.org/10.1063/1.4840395.

(16) Stamatakis, M.; Vlachos, D. G. A Graph-Theoretical Kinetic Monte Carlo Framework for on-Lattice Chemical Kinetics. *J. Chem. Phys.* **2011**, *134* (21), 214115. https://doi.org/10.1063/1.3596751.